BNL--42812

DE89 012975

UV PHOTOEMISSION FROM METAL CATHODES FOR PICOSECOND POWER SWITCHES*

CONF-8810135--5

J. Fischer, T. Srinivasan-Rao and T. Tsang

Brookhaven National Laboratory
Upton, New York 11973, U.S.A.

ABSTRACT

Results are reported of photoemission studies using laser pulses of 10 ps duration and 4.66 eV photon energy on metal cathodes. These included thin wires, flat surfaces and an yttrium cathode with a grainy surface.

The measurements of current density and quantum efficiency under low and high surface fields indicate that field assisted efficiencies exceeding 0.1% and current densities exceeding 10^5 A/cm^2 are obtainable. The results are compared to the requirements of switch power applications.

INTRODUCTION

Novel accelerator concepts such as the Switched-Power Linac (SPL), originally proposed by W. Willis,[1] and pulsed power sources such as the microlasertron proposed by R. Palmer,[2] call for fast switches with current densities exceeding 100 kA/cm^2 from a 1 cm^2 area with electron bunch lengths of the order of a few picoseconds at fields of 10^7 to 10^9 V/m. In addition a variety of proposed high energy accelerators[3] and the Accelerator Test Facility (ATF)[4,5] at BNL, as well as coherent picosecond x-ray FELS require electron bunches of extremely low emittance, short duration, high current density and high brightness.

---

*This research was supported by the U. S. Department of Energy: Contract No. DE-AC02-76CH00016.

Such e^- sources must be efficient, rugged, and able to operate at high repetition rates. It is difficult to meet these requirements with conventional electron sources. However, photocathodes driven by short, intense laser pulses are more suitable for these applications, since the electron density and pulse length can be controlled by the laser intensity and pulse width. Cesiated metal and semiconductor cathodes,[6,7] which have been studied in recent years, have high quantum efficiency, but require vacuum below 10^{-10} Torr, in situ preparation, and have a short life due to surface degradation and poisoning. Metal cathodes, on the other hand, can be rugged, relatively stable to brief exposure to air, can operate in moderate vacuums and have a long life. Also, the high density of electrons in the conduction band of metals, and their low resistivity, is conducive to high current density photoemission. However, the quantum efficiency of simple metals is relatively small and require UV illumination for photoemission.[8-12]

Some of our measurements of quantum efficiency and high current density for metal photocathodes with 10 ps UV laser pulses have been reported previously.[8,10] Here we summarize these results and report on our experiments to improve the quantum efficiency by suitable choice of metals, activation of the surface with UV laser pulses, and field assisted reduction of the effective work function and with applied fields enhanced by a thin wire or by a grainy cathode surface. The results are discussed in relation to SPL applications. The experiments were done under "practical" laboratory conditions as expected at accelerators.

Figure 1 illustrates the similarity of our photodiode arrangement to the design of an SPL. Figure 1(a) shows a schematic cross section of the ring shaped photodiode in the gap between the first two discs of an SPL.[13] Figure 1(b) indicates our experimental flat photodiode which simulates a small portion of the SPL ring cathode. However, the applied fields in our measurement were below 3×10^7 V/m DC, whereas in the SPL a prepulse with 5 to 10 times higher fields will energize the ring photocathode. The photocathode in the electron bunch source of the SPL may experience fields of the order of 10^9 V/m.

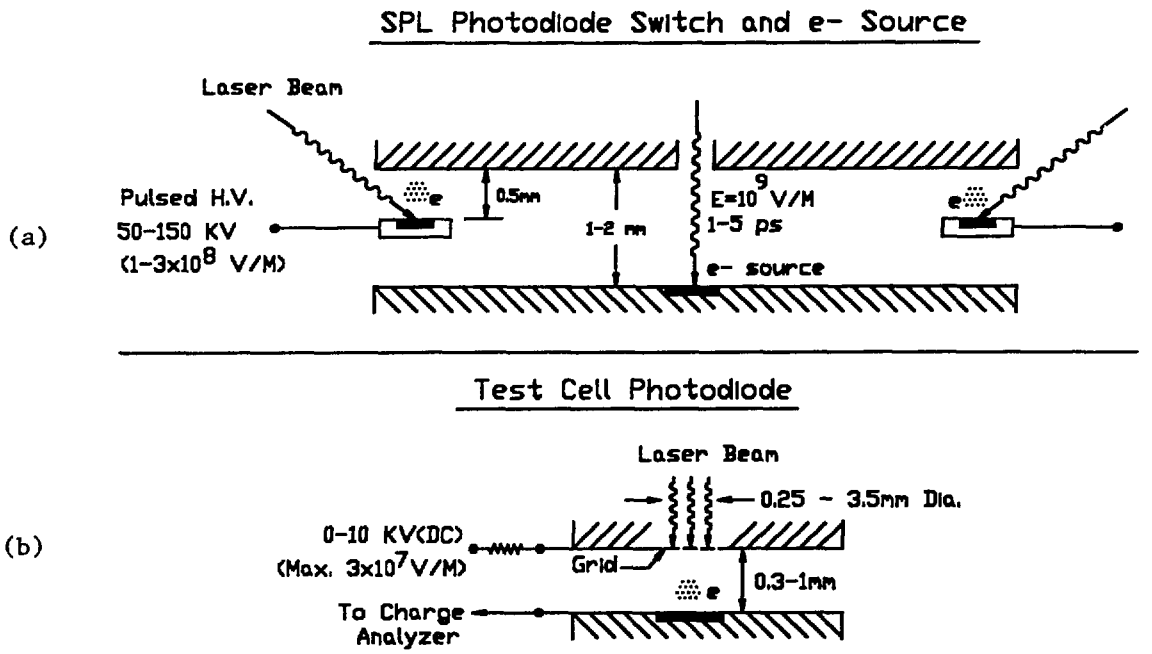

Fig. 1 (a) Schematic of the cross section of a single ring photodiode switch of an SPL with the electron source in the middle. The diagram is not drawn to scale.

(b) Schematic of the electrode configuration in our experimental arrangement.

EXPERIMENTAL ARRANGEMENT

The schematic of the experimental arrangement is shown in Fig. 2. The output of a frequency quadrupled, active and passive mode-locked Nd:YAG laser (Quantel YG 501) was passed through a series of variable irises, and attenuators to yield a laser beam of well defined energy and spot size at the cathode. The energy of the beam entering the target cell can be measured by directing the beam into a joulemeter (Molectron J3) with the movable mirror M. A small portion of the laser beam reflected from a CaF_2 beam splitter was directed onto a one dimensional vidicon to monitor the spatial profile of the laser beam.

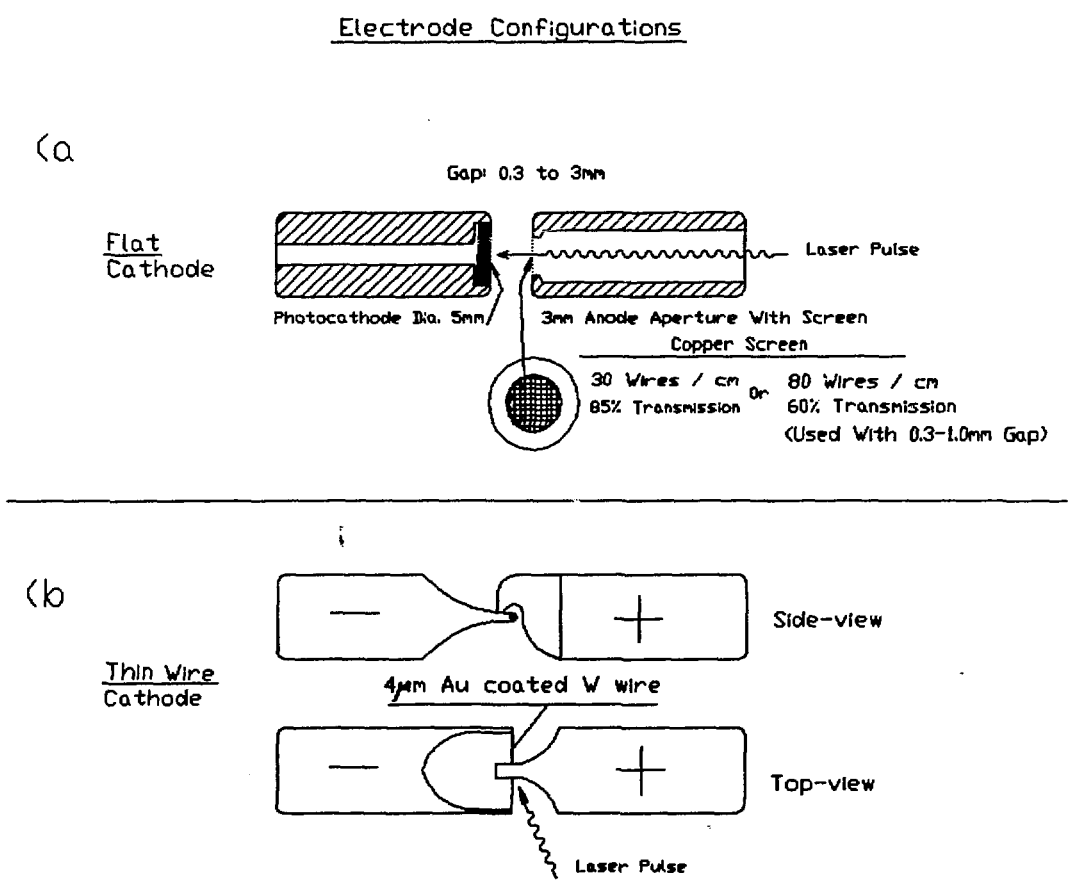

Fig. 3 Schematic of the electrode configuration.

(a) for a flat cathode held at a variable distance from a hollow anode, covered with a fine mesh.

(b) for a 4 μm wire held coaxially to the anode. The laser beam can illuminate up to 500 μm length of the wire held under the anode.

In the second arrangement, the photocathode, consisting of a 4 μm diameter gold coated tungsten wire, was held in the center of a surrounding anode in a coaxial geometry (Fig. 3(b)) with an electrode gap of 1 mm. Such thin wires give rise to high surface electric fields. Surface field enhancements of about 1000 over the applied voltage were obtained. The wire was illuminated obliquely so that the field lines at the emitting area would not be distorted significantly.

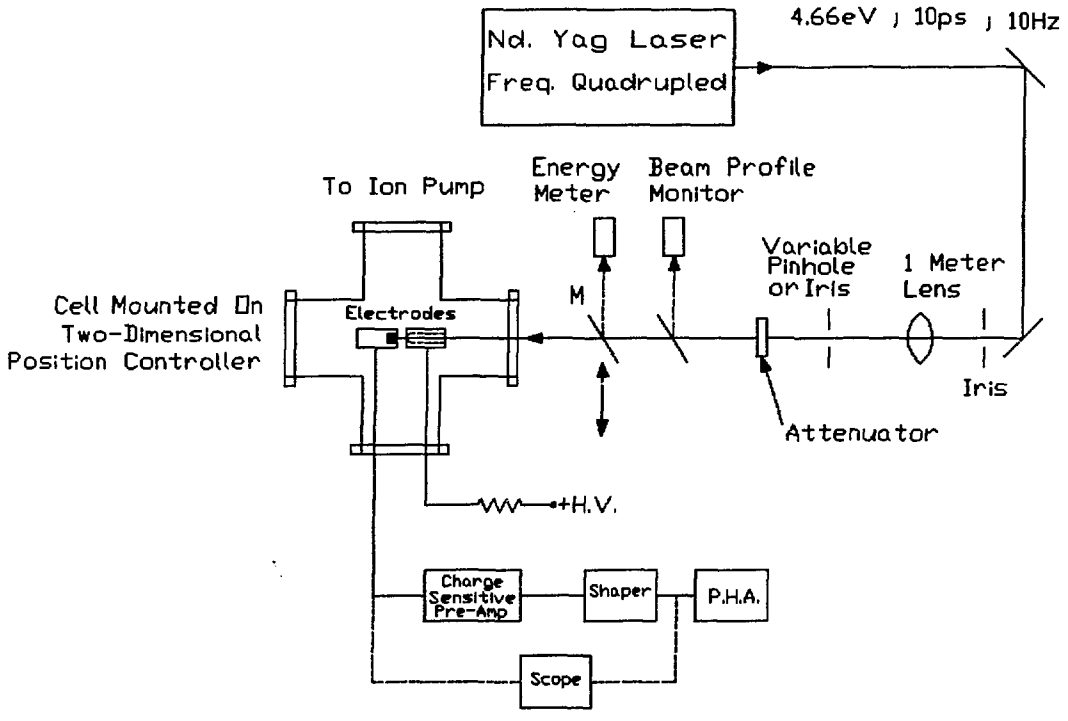

Fig. 2 Schematic of the experimental arrangement.

The target cell consisted of a stainless steel six-way cross mounted on a remotely controlled x-y translation stage of 1 μm resolution. The UV beam entered the cell via a sapphire window. The pressure in the cell can be maintained in the range 10^{-8} - 10^{-9} Torr with turbo and ion pumps.

Two different diode configurations were used in the measurements. The arrangement using flat electrodes is shown in Fig. 3(a). The electrodes were arranged in the middle of the cell with their surfaces parallel to each other. The cathode was illuminated at normal incidence by the laser light passing through the hollow anode of 3.9 mm inner diameter. The anode surface facing the cathode was covered by a wire mesh. The electrode gap was variable from 0.3 to 3 mm. The gap and mesh size were chosen so that the field lines at the emitting area would not be distorted significantly by the wire mesh. DC voltages up to 10 kV can be applied to the anode via a resistance of 50 MΩ.

The information about the electron emission was derived directly from the cathode as shown in Fig. 2. The output was fed into a calibrated charge sensitive preamplifier, shaping amplifier and pulse height analyzer. The fluctuations in the laser energy was monitored and the electron yield was normalized accordingly.

PHOTOCATHODE PREPARATION

The gold coated tungsten wire cathode, in its fork-like holder, was washed with solvents and cleaned in hexane before insertion into the vacuum test cell.

The flat photocathodes were made of small sheet metal discs, machined from the desired metals. The discs were attached to the copper electrodes. The combined cathode and electrode surface was then lapped with a 1 μm diamond compound, washed in solvents and ultrasonically cleaned and stored in hexane topped with N_2. The electrodes were assembled and treated under practical conditions to be expected at accelerators. When setting the electrode gap on a measuring machine, there was a brief 1-2 minutes exposure to air, while wet with hexane. The assembly was then cleaned with a N_2 jet and installed in the test cell in a N_2 atmosphere. The cell was then evacuated, baked at ~150°C, and pumped to a pressure of a few 10^{-9} Torr at room temperature.

To activate the photocathode, a 3 mm dia of the cathode surface is irradiated with the 266 nm UV laser beam, usually of 3-5 mJ/cm^2, for 5-10 minutes before each experiment. We observed that:

- The quantum efficiencies increased, in some cases, up to four orders of magnitude, after activation by the laser beam.
- There seemed to be a minimum laser intensity required for the activating process. The efficiency also increased with the number of laser pulses before it stabilized. Longer activation times and much higher intensities damaged the surface.
- 532 nm laser beams were much less effective.
- During activation the pressure in the cell increased.
- The efficiencies decreased slowly with time, when the cathode was not strongly illuminated during the experiment.
- If the vacuum was poor, the efficiency decreased faster.

- A usable operating time was ~6 hours at 2-3 × 10^{-9} Torr for a 10-30% decrease in yield depending on the sample. The cathode could be rejuvenated by reirradiating the surface as described above for 5 min. The deterioration could be attributed to the formation of layers of residual gas molecules on the cathode surface. A useful time of 24 hours or more may be obtained with a vacuum of about 10^{-10} Torr.

QUANTUM EFFICIENCIES (η) AND WORK FUNCTIONS (ϕ) OF METAL PHOTOCATHODES

The quantum efficiency η, defined as the number of emitted electrons per incident photon on the cathode, can be written as

$$\eta = \frac{\text{emitted charge (Coulombs)}}{\text{incident laser energy (Joules)}} \times \text{Energy of Photon (eV)} \qquad (1)$$

To calculate the efficiency of the metals, for a given incident energy, the charge emitted from the cathode is measured for various electric fields. The charge, obtained for a field large enough to overcome space charge effects, but not yet large enough to alter the work function, was used in Eq. (1). Plots of yield versus field are shown in Fig. 4 for Y, Mg, and Sm.

The quantum efficiencies derived from our measurements for Au, Ta, Mg, Ti, Y and Sm are listed in Table 1 together with corresponding published values of work function (ϕ) for the elements[14] and for MgO.[15] As expected η generally increases with decreasing work functions.

It is worth noting that all the photocathode surfaces were activated by irradiation with a UV beam. The activation procedure could have altered both the chemical composition and the structure of the surface. The actual work function of these surfaces could be different from the published values. No attempt was made to study either the chemical composition or the surface structure of these surfaces in detail. Furthermore the cathode surfaces were not highly polished.

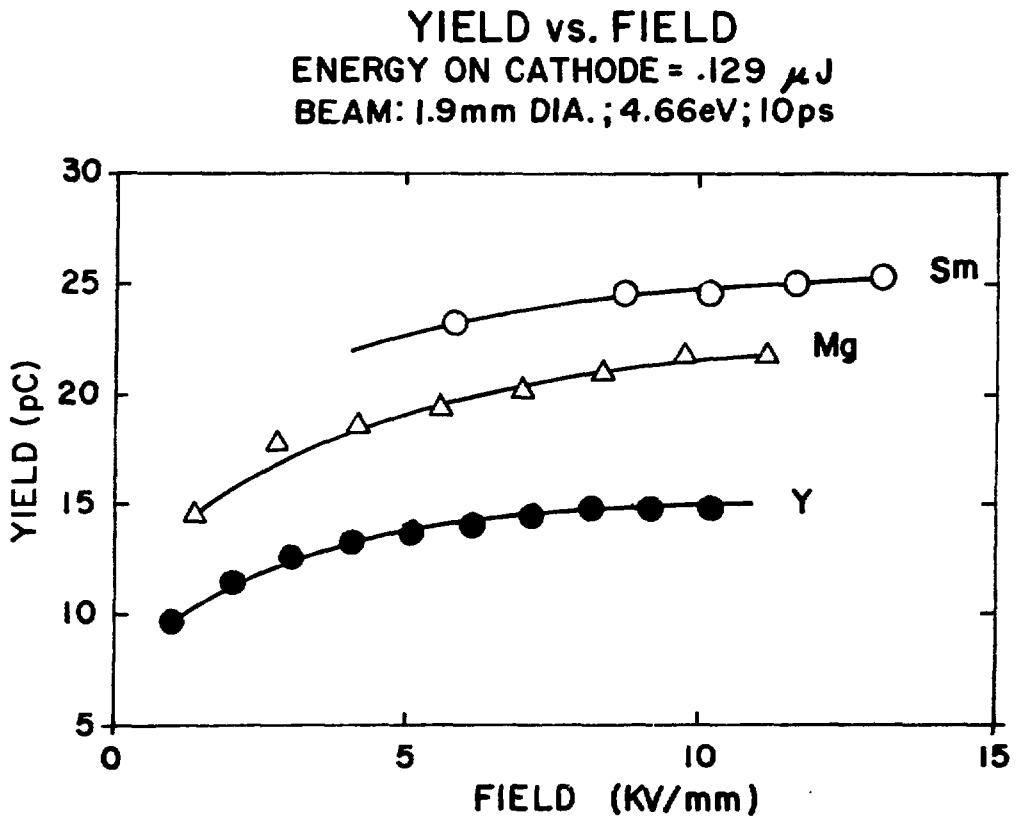

Fig. 4 Yield vs field curve for Sm, Mg and Y. Laser parameters are photon energy 4.66 eV, pulse duration ~10 ps, pulse energy 129 nJ, 1.9 mm dia. At low fields, space charge effects predominate. For fields above 5 kV/mm, the emission is determined by the pulse energy of the laser and the effective work function of the material.

The presence of protrusions could have generated high local surface fields that might alter the effective work function. Gold in the form of a wire, of sheet metal, or as an evaporated layer, gave a higher η than expected. Similar efficiencies have been observed by others.[16] Insufficient cleaning of Ta and Te may be the cause of deviation from their expected behavior.

The dependence of the quantum efficiency on the work function is illustrated in Fig. 5, where the measured values of η are plotted versus $(h\nu-\phi)^2$. $h\nu$ is the energy of the photon

Table I. Published Work Functions and Observed Quantum Efficiencies*

Material	Work Function ϕ (eV)	Measured Efficiency, η 10^{-3}
Gold	5.1	.047
Tantalum	4.25	.01
Magnesium	3.66	.62
Yttrium	3.1	.5
Terbium	3.0	.235
MgO	2.9	.62
Samarium	2.7	.725

*Electrons emitted per incident photon.
**Probably MgO

and ϕ is the work function of the metal. As expected[17] there is an approximate linear relationship between η and the square of the excess energy of the photon above the work function.

$$\eta \approx K(h\nu-\phi)^2 \tag{2}$$

A line drawn from the origin through our measured efficiencies for MgO and Y, indicates a slope of $K \approx 2 \times 10^{-4}$. However, K is dependent on the photon absorption which is subject to surface roughness, temperature and wavelength. Other factors that affect K are crystal structure, density of state, transition probability, angle of photon incidence, polarization of the photons, etc.

Theoretical description and experimental results concerning the improvement of the efficiency by field assisted photoemission and by surface structures are discussed in later sections.

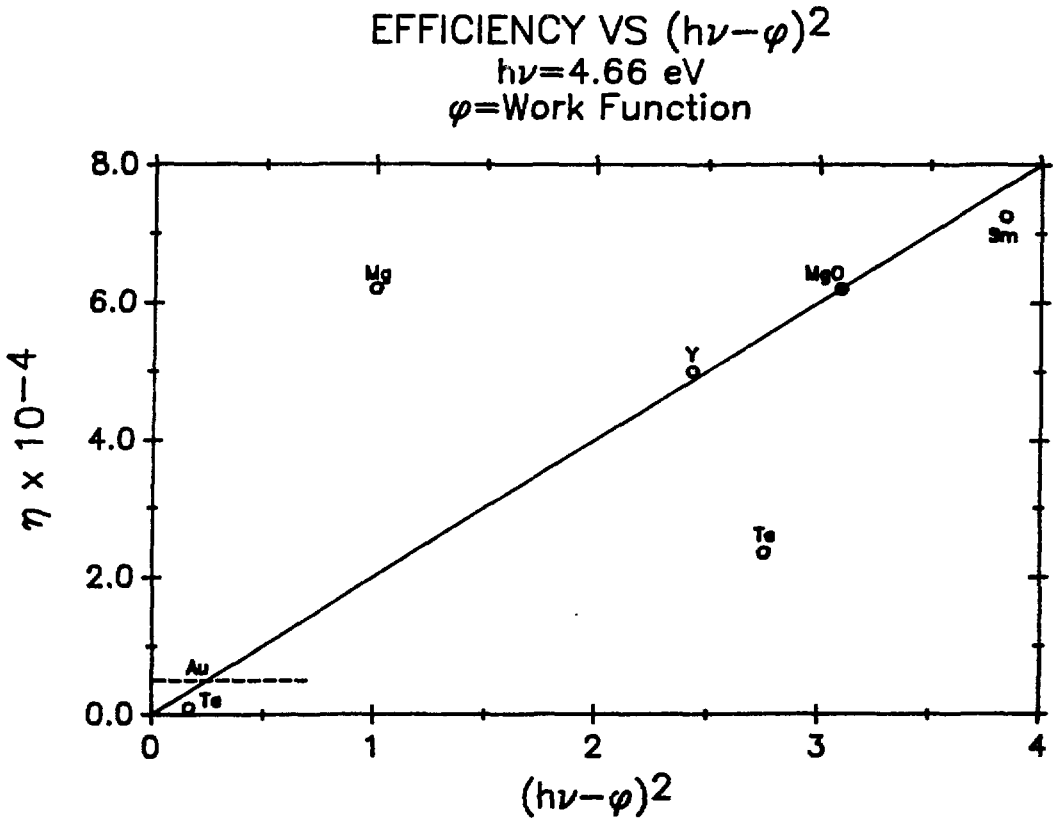

Fig. 5 Efficiency of different metals is plotted against the corresponding $(h\nu - \phi)^2$ where $h\nu$ = 4.66 eV and ϕ is the published work function of the metal. The solid line corresponds to $\eta = 2 \times 10^{-4}(4.66 - \phi)^2$. Efficiency of gold is indicated by the dashed line.

HIGH CHARGE AND CURRENT DENSITIES

The current density of photoemission from metal cathodes can be very high. Peak emission of the order of 10^9 A/cm^2 from very sharp needle points have been reported.[18] However, emission densities from macroscopic areas are subject to practical limitations such as space charge effects, optical surface damage, and field breakdown. Field breakdown can also be triggered by local gas or vapor desorption from the cathode by the laser pulses and by the photoemission process. The light intensity has to be well below surface plasma formation levels.

Figure 6 illustrates the dependence of yield and current density on the field for samarium, with a light pulse energy of 1.1 μJ on .05 mm^2 spot. It can be seen that the maximum field of 13 kV/mm is barely sufficient to overcome the space charge effects. The yield of 170 pC corresponds to a current density of ~34 kA/cm^2.

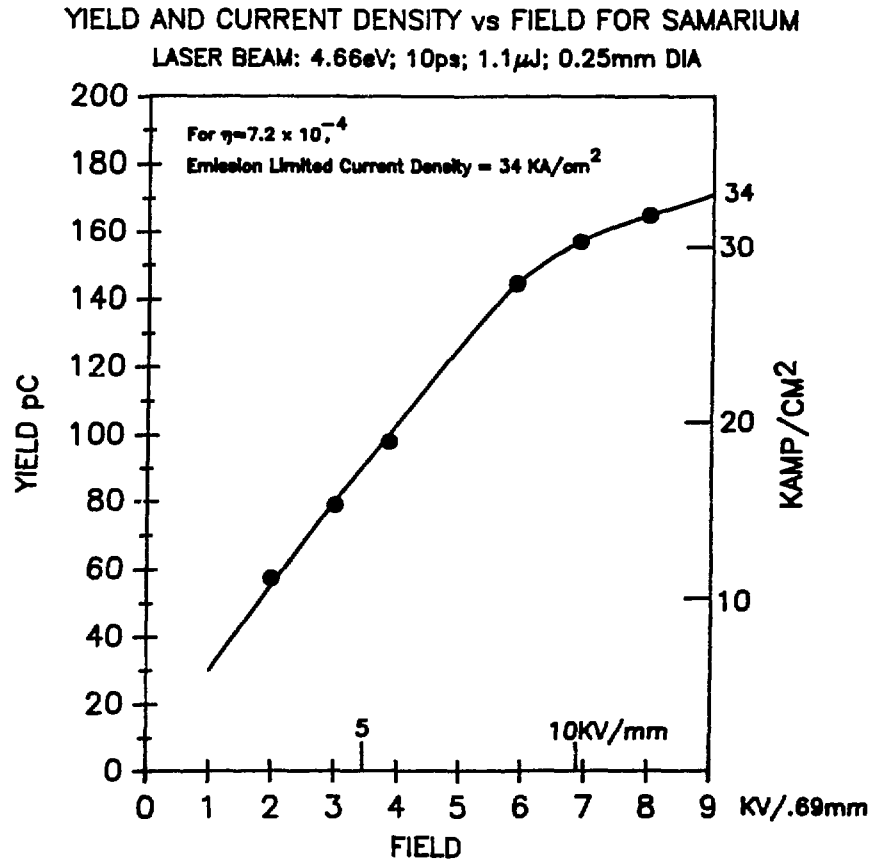

Fig. 6 Charge and current density from samarium plotted as a function of the applied field. At fields of 10 kV/mm, emission limited operation is barely beginning. Maximum current density obtained for 1.1 μJ UV laser energy on a 0.25 mm dia spot is ~34 kA/cm^2.

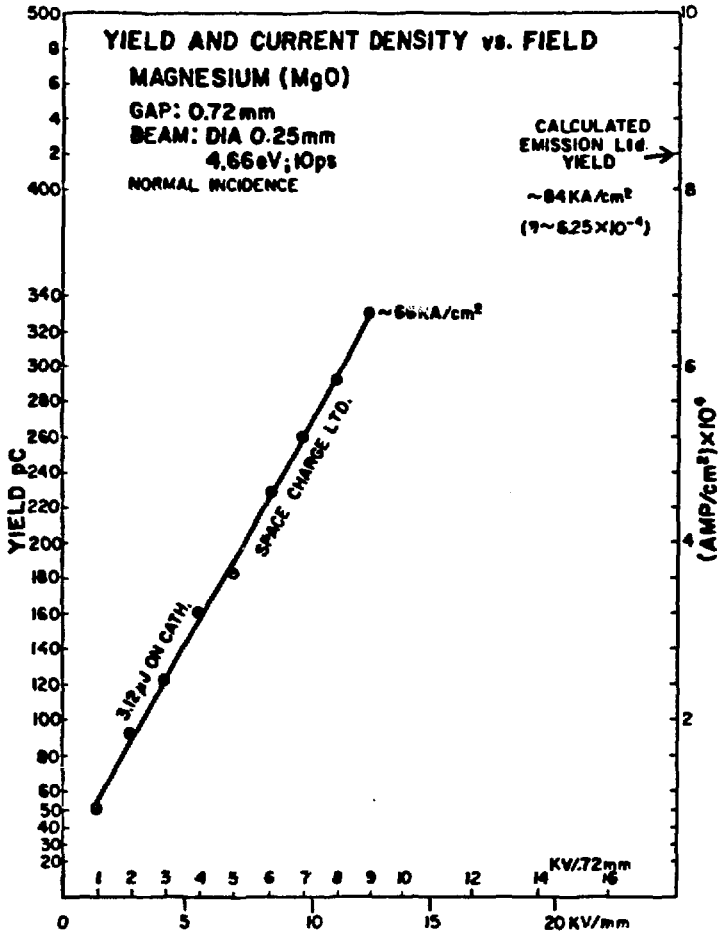

Fig. 7 Charge vs field plot for Mg. The scale on the right is the corresponding current density in a space charge free regime (where electron pulse duration equals laser pulse duration). Even at the maximum field applied, the emission is space charge limited. If it was space charge free, the expected current density, for a laser energy of 3.1 μJ on 0.25 mm dia spot and an efficiency of 6.25×10^{-4}, would be ~84 kA/cm^2.

Figure 7 is a similar plot for a magnesium cathode illuminated with a more intense laser pulse of 3.1 μJ. The emission is space charge limited even at the maximum applied field. Under these conditions the charge increases linearly with the field, i.e., $Q \propto V \times C$.

At the maximum field applied, the measured charge was about 330 pC, which implies a current density of 66 kA/cm^2 assuming a pulse duration of 10 ps. Based on our previously measured quantum efficiency of 6.25×10^{-4}, the emission limited current density for this light pulse energy would be 84 kA/cm^2, if the field were high enough (estimated >25 kV/mm) to be free of space charge. As will be shown later, for the high fields to be used in SPL, the field assisted efficiencies may exceed 0.1% for yttrium. From these examples and corresponding results with yttrium, it is apparent that current densities exceeding 10^5 A/cm^2 can be obtained at higher fields.

The laser damage threshold would limit the attainable current density for a given quantum efficiency. In the case of yttrium such threshold, currently under investigation, is about 10 mJ/cm^2.

FIELD ASSISTED PHOTOEMISSION

A. An Overview.

The energy required for electrons in their highest energy state (Fermi level at absolute zero) to escape from the metal into the vacuum is called the work function ϕ, and is equal to the height of the potential barrier. At temperatures above absolute zero, the electrons in the metal have a thermal energy distribution and require correspondingly less energy to escape from the metal. In simple photoemission, this energy has to be supplied by the photon. Any excess energy of the photon over the work function appears as the kinetic energy of the escaping electron, and can make the emittance worse.

The application of the electric field affects extraction of photoelectrons in various ways. Figure 8 is a diagrammatic representation of the variation of yield with the applied field, for a constant illumination. In region 1, the applied field is so low, that the space charge effects are predominant. As the field is increased, the space charge effects are overcome and in region 2, the emission is controlled by the photon flux. In this emission limited regime, the modification of the potential barrier due to the electric field is not significant. Intrinsic (no enhancement due to the field) photoemission quantum efficiency can be measured in this regime.

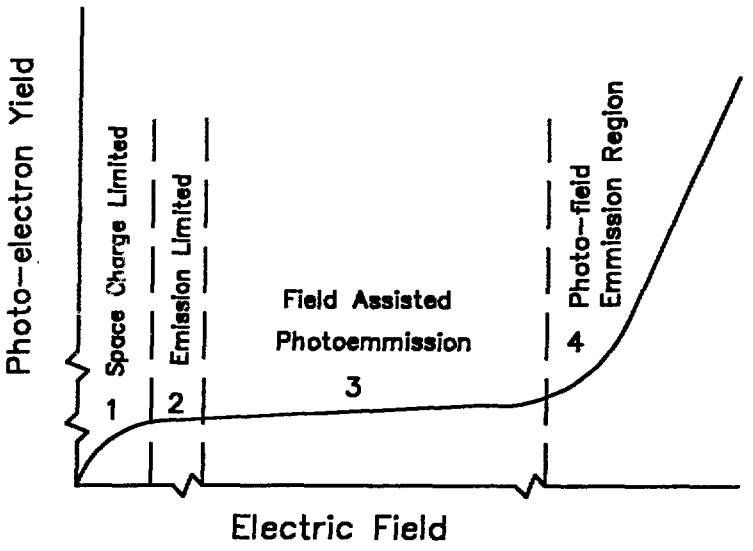

Fig. 8 Diagrammatic representation of the dependence of the photoelectron yield on the field in 1) space charge limited, 2) emission limited, 3) field assisted photoemission, and 4) near the dark field emission regime. See text for more detail.

For fields in the range 10^6-5×10^8 V/m, (region 3) the height and width of the potential barrier between the Fermi and vacuum levels are modified. The reduction in the width of the barrier is not large enough in this regime to contribute significantly to electron emission. The reduction in the height, however, is equivalent to a lowering of the effective work function (Schottky effect),[19] resulting in an increase in the quantum efficiency. In this regime, the electron emission is still controlled by the incident photon, and is referred to as the field assisted photoemission. SPL, microlasertron and RF driven electron guns, operate at these fields.

As the field is increased further, the contribution due to the narrowing of the barrier increases, since electrons can tunnel through the barrier with increasing escape probability (Fowler & Nordheim).[20,21] The photoelectron emission in this region (photo-field emission, region 4) is high,[18] but at these high fields it may not be completely controlled by the photons. The work function approaches zero on further increase in the field, ushering in the dark field emission regime.

Fields exceeding 10^8 V/m require fast (sub nanosecond) electrical pulses to prevent electrical break-down on smooth metal electrodes. However, surface fields exceeding 10^8 V/m can be realized with DC fields, if the surface is not smooth, but covered with microscopic protrusions produced intentionally or by chance. Significant field emission dark currents from photocathodes should be avoided because of stability and breakdown problems. The duration of photoemission in the photo-field emission region may exceed that of the laser pulse.

The presence of a thin layer of adsorbed oxides or particulates may also lower the effective work function, due to tunneling from the metal and band bending in the particulates, and therefore enhance the emission, at fields which are lower than for the plain metal alone.[22] In practical cathodes of macroscopic areas, a mixture of all the processes mentioned in the preceding paragraphs can be present.

B. Efficiency, Schottky Effect, and Field Enhancement

In the field assisted photoemission regime the effective work function ϕ_1, due to the Schottky Effect, can be written as:

$$\phi_1 \approx \phi_0 - \left(\frac{e}{4\pi\epsilon_0}\right)^{1/2} \times E_s^{1/2} \qquad (3)$$

where

$$\left(\frac{e}{4\pi\epsilon_0}\right)^{1/2} \simeq 3.786 \times 10^{-5} \text{ in MKS units}$$

ϕ_0 = work function. The subscript "zero" is used from here on to emphasize zero field, e = charge of the electron, ϵ_o = dielectric constant of free space, E_s = surface field.

The surface field E_s is a product of the applied field and a field enhancement factor β due to geometrical factors, surface roughness, etc. Equation (2) can now be expressed as a function of an applied field E by substituting the expression for ϕ_1 in place of ϕ. For photons of 266 nm this results in

$$\eta \approx K\,[4.66 - (\phi_0 - 3.786 \times 10^{-5}\sqrt{\beta E})]^2 \qquad (4)$$

K and β are considered to be field independent. The slope and y-intercept of the straight line plots of $\sqrt{\eta}$ vs $\sqrt{E}$, gives $\sqrt{K\beta}$ and $\sqrt{K}\,(h\nu - \phi_0) = \sqrt{\eta_0}$, respectively. If any one of the three unknowns (K, β and ϕ_0) is already known, the other two unknowns can be calculated from these slope and intercept measurements. Alternatively, the data points can be fitted to Eq. (4) by a least square method with K, β and ϕ_0 as parameters and the best fitting set can be chosen to represent the surface.

The increase in efficiency in the field assisted regime is illustrated in Fig. 9 as a theoretical plot of $\sqrt{\eta}$ vs $\sqrt{E}$ with $K = 2 \times 10^{-4}$, $\beta = 1$, $h\nu = 4.66$ eV, and ϕ_0 ranging from 2.7 to 4.2 eV. The published work function of Sm, Mg, and Y fall within this range. The y-intercept of the lines give $\sqrt{\eta_0}$ for each ϕ_0. The dashed line on this figure corresponds to $\eta = K \times 4.66^2$, i.e., where the effective work function $\phi_1 = 0$ considering the Schottky effect only. The field at which $\phi_1 = 0$ for a given ϕ_0 can be obtained from the x-coordinate of the point of intersection of the dashed line and the corresponding $\sqrt{\eta}$ vs $\sqrt{E}$ line. These limiting surface fields would of course increase with metals of higher work function, which may be useful in applications where extreme fields are expected.

At a field of 10^9 V/m, η_0 increases by factors of about 2.5 and 9 for ϕ_0 values of 2.7 and 4.2 eV, respectively, due to the Schottky effect. The real increase may be higher because of the onset of significant tunnelling at fields of 10^9 to 10^{10} V/m, where the Schottky formula is insufficient.

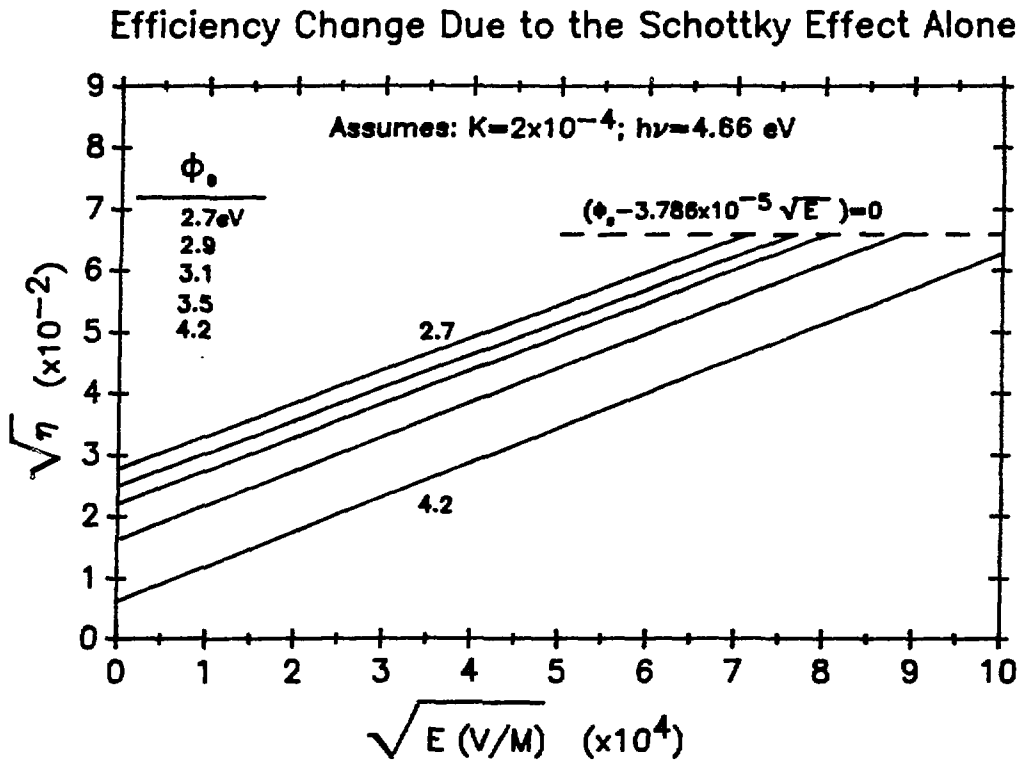

Fig. 9 $\sqrt{\eta}$ calculated using Eq. (4) is plotted as a function of $\sqrt{E}$. The parameters used are $K = 2 \times 10^{-4}$, $\beta = 1$ and ϕ_0 ranging from 2.7 to 4.2 eV. The y-intercept for each line is $\sqrt{\eta_0}$ corresponding to that ϕ_0. The dashed line corresponds to $\phi_0 = 3.786 \times 10^{-5} \times \sqrt{E}$ and $\eta = 4.3 \times 10^{-3}$. As this field is approached, the effective work function vanishes, the electron emission approaches field emission, and Eq. (4) is not valid anymore.

C. Experiments

We describe two experiments to measure the field assisted photoemission using low intensity laser light pulses of 266 nm (4.66 eV) of 10 ps FWHM duration.

In the first experiment a 4 μm dia gold coated tungsten wire was held 1 mm from an anode in a coaxial geometry as shown in Fig. 3(b). In such a case the approximate field enhancement can be calculated from the geometry, and the applied voltage, by the well known formula

$$E_{surface} = \frac{V}{r \ln R/r} \qquad (5)$$

where r and R are the radii of the cathode and anode. For the physical parameters used in this experiment, the enhancement is $\approx 10^5$, if E is expressed in V/m, and thus permits investigation of high surface fields with modest applied D.C. voltages.

From our experimental measurements of yield for various applied voltages, the efficiency can be calculated as a function of the surface field. In this experiment the maximum surface field was 3×10^8 V/m.

Figure 10 illustrates the relation of $\sqrt{\eta}$ vs $\sqrt{E_{surface}}$. The field assisted efficiency at 3×10^8 V/m increased by about a factor of six over η_0. From the slope and the y-intercept of the extrapolated line through the data points, the value of K and ϕ_0 can be calculated using Eq. (4), and substituting $E_{surface}$ for βE. One obtains $K \approx 9.8 \times 10^{-6}$ and $\phi_0 \approx$ 4.2 eV. This ϕ_0 for gold is lower than a reported value of 4.68 eV.[23] However, our vacuum and surface conditions were not perfect.

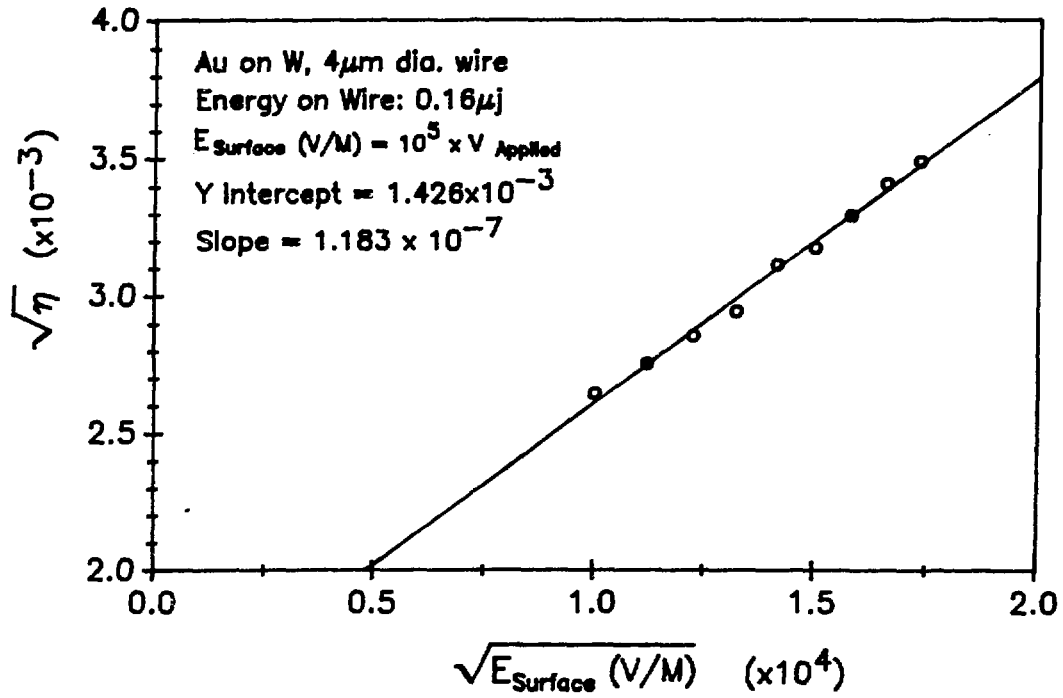

Fig. 10 The experimental efficiency versus surface fields up to 3×10^8, using a 4 μm dia gold coated tungsten wire cathode, as in Fig. 3(b). The slope and y-intercept of the extended line through the data points determines the constants of Eq. (4) for this case.

In the second experiment a flat yttrium cathode was used in the configuration shown in Fig. 3(a). The experimental parameters are: laser energy 37.5 nJ, spot size 0.25 mm dia, electrode gap 0.425 mm, anode wire screen 80 wires/cm. The presence of this screen modifies the intensity distribution of the laser beam due to diffraction. This modification, as well as hot spots in the original laser beams resulted in local peak intensities estimated at 30-60 mJ/cm^2 during the activation treatment. This feature caused an interesting surface damage or graininess as will be shown later.

The results of the measurements plotted as $\sqrt{\eta}$ versus $\sqrt{}$applied field are shown in Fig. 11 for applied fields up to 2.5×10^7 V/m. It shows a stronger increase of η with the applied field than expected for a smooth cathode. The expression of Eq. (4) was then fitted to the data points in the emission limited linear region by a least square method. The best fitting parameters are: $K \simeq 2 \times 10^{-4}$; $\phi_0 \simeq 3.3$ eV and an average field enhancement factor of $\beta \simeq 20$. For comparison $\sqrt{\eta}$ calculated for $K = 2 \times 10^{-4}$, $\phi_0 = 3.3$ eV but $\beta = 1$, as a function of $\sqrt{E}$, is also shown in Fig. 11. It results in a much smaller increase with the applied field. Preliminary experiments with uniformly activated fresh yttrium surfaces indicate that the ϕ_0 for such surface is 2.9 eV. Nonuniform activation and degradation of the surface during the elapsed time between activation and measurement could be the cause of higher ϕ_0 in this measurement.

For a more uniformly activated fresh yttrium surface, the data points would follow the upper line calculated for $\phi_0 = 2.9$ eV, and $\beta = 20$.

An extrapolation of this line to an applied field of 10^8 V/m, the operating field for the SPL, would indicate an efficiency of 2.4×10^{-3}. Because of the high surface field this value is also expected to be increased substantially by electron tunneling effects.

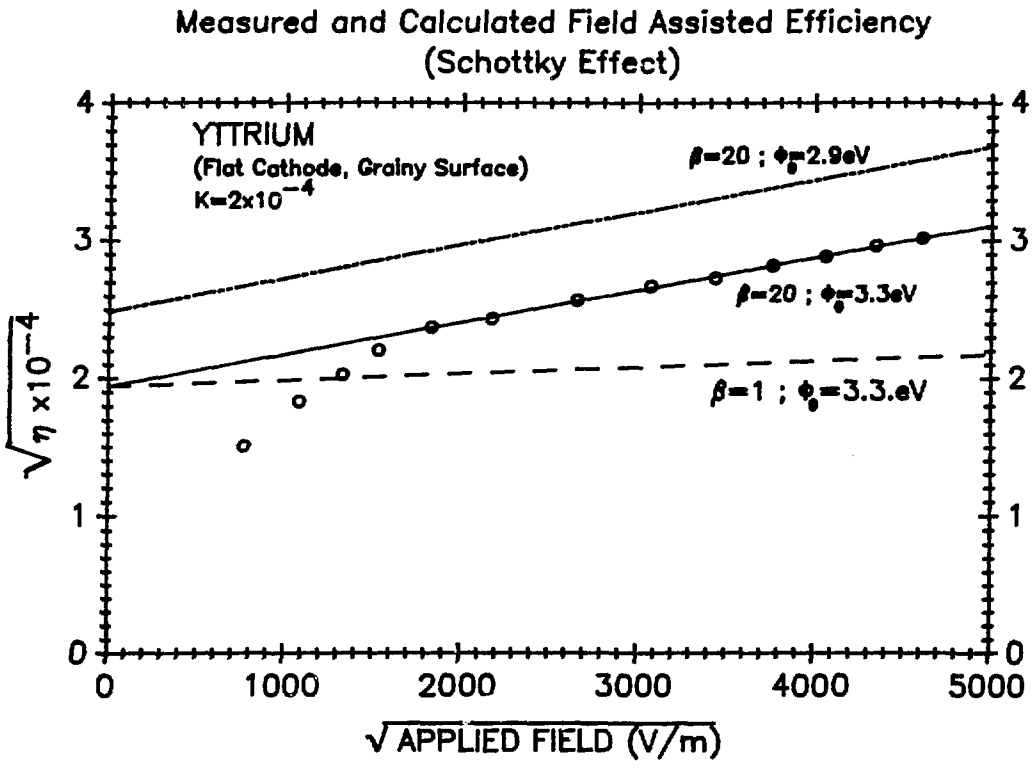

Fig. 11 $\sqrt{\eta}$ vs $\sqrt{E}$ for a flat Y cathode. Circles are experimental data points. Least square fit to the data results in $\beta = 20$, $\phi_0 = 3.3$ eV and $K = 2 \times 10^{-4}$. The dashed line is $\sqrt{\eta}$ calculated from Eq. (4) with $\beta = 1$, $\phi_0 = 3.3$ eV and $K = 2 \times 10^{-4}$. The top line is $\sqrt{\eta}$ calculated from Eq. (4) with $\beta = 20$, $\phi_0 = 2.9$ eV and $K = 2 \times 10^{-4}$.

D. Grainy Cathode Surface by UV Activation

The SEM photographs of an yttrium cathode surface activated with a UV beam passing through the fine wire mesh of the anode are shown in Fig. 12 a, b, and c, with increasing magnifications of 12, 430 and 4300. The activation was done with a 3 mm dia beam through the anode screen for 10-20 minutes, at peak intensities of 30-60 mJ/cm^2 on the cathode surface, as mentioned above. The overall view in Fig. 12(a) shows the shadow of the anode screen wires superimposed on the damaged surface, thus dividing this area

in little squares. An enlarged view of several of these squares is shown in Fig. 12(b). The bright and darker stripe pattern in each square is caused by the intensity modulation in the laser beam due to diffraction by the screen. Further enlargement of the area near the edge of such a square is shown in Fig. 12(c) which reveals the grainy character of the surface, probably caused by repeated recrystallization of the yttrium, after flash melting during the 10 ps, 10 Hz, laser pulses. The grain size increases with the intensity, in the diffraction pattern. One would expect about 40% intensity variation between the brightest first maximum and its neighboring minimum, which shows much smaller grains.

The effect on the anode, shown in Fig. 13(a), shows a darkened area, when viewed from the cathode side. A magnified portion of the grid wires shown in Fig. 13(b) reveals details of the darkened area, identified as deposits of evaporated or ablated yttrium, by electron probe x-ray analysis.

In these measurements, the size of the test beam, positioned for maximum efficiency, covered simultaneously 4 - 9 of the squares shown in Fig. 12(b). The test beam followed the same diffraction pattern as the activating beam, i.e., the highest intensity is incident on the larger grains. The field intensification factor β found from our data is therefore a weighted average value. The local β may vary within the pattern of each square.

It is difficult to calculate accurately the enhancement factor from the appearance of the grains, since they vary in size and edge sharpness. The SEM also does not show the height of the protrusions above the surface. The production of more uniform grainy surfaces under controlled conditions without the diffraction pattern, and determination of the resulting β, ϕ_0, η and grain size, as function of the UV activation are currently under investigation.[24]

RESULTS AND THEIR RELEVANCE TO HIGH POWER SWITCHES

These experiments indicate that strong UV activation of metal cathodes, e.g., Y, Mg or Sm give rise to grainy surfaces which enhance the surface field over the applied field. For applied fields of 1-3 $\times$ 10^8 V/m, (operating fields in pulsed power switches), the calculated field assisted efficiency may exceed 0.1% due to this enhancement.

b)

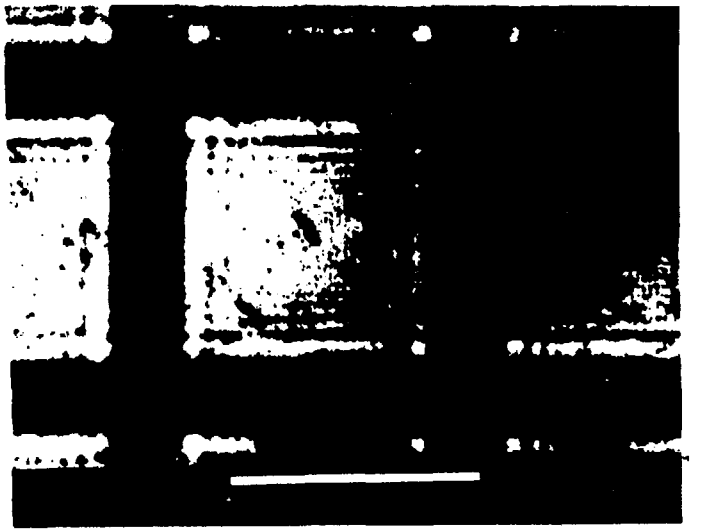

a) **Polished yttrium cathode after localized exposures to laser light pulses via anode grid 0.425 mm away. Laser: 266 nm, 10 ps, 10 Hz, 10-20 minutes. Grid: wire 15 μm; spaces 112 μm.**

b) **Diffraction pattern of the anode grid on the cathode.**

c) **Detail of surface changes within the diffraction pattern.**

Fig. 12 Surface details of UV activated yttrium cathode.

c)

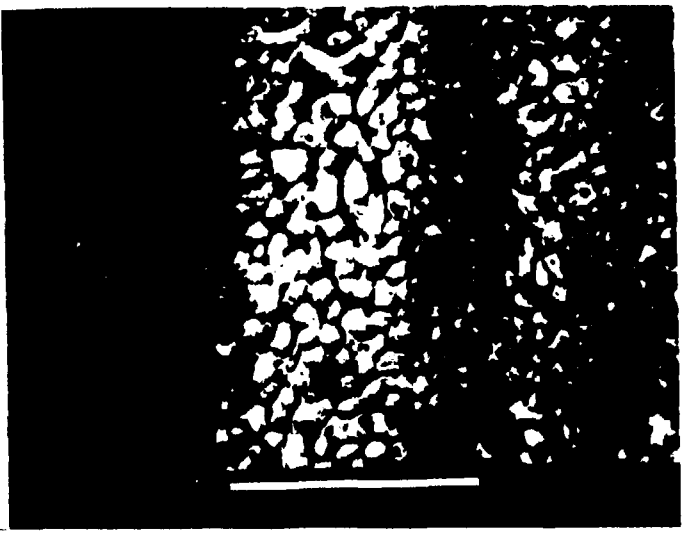

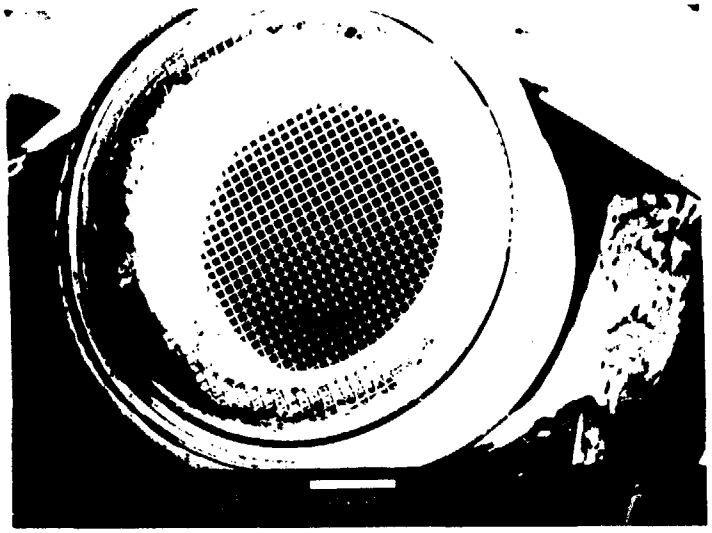

Hollow anode (~4 mm I.D.) with copper grid facing yttrium cathode at 0.425 mm distance.

Grid wires 15 μm
Open spaces 112 μm

Note dark area (upper left) where strong laser beam passed.

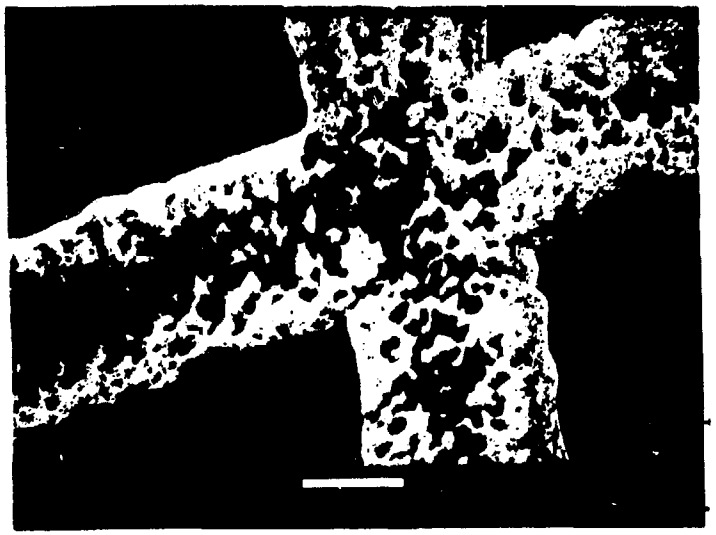

Detail of dark area showing deposit of yttrium (opposite cathode damage).

Fig. 13 SEM photograph of the anode and anode screen. Details as noted on the photograph.

In these experiments, the maximum measured current density of 60 kA/cm^2, was limited by space charge effects. However, in the high power switches, where the applied field may exceed 10^8 V/m, the limiting mechanism may be the optical damage of the cathode by the laser irradiation and not the space charge effect. An efficiency of 0.2% and a laser pulse width of 10 ps would permit a current density of ~200 kA/cm^2 and still have a damage threshold safety factor of 2. Higher current density without significant damage may be obtained by using lasers of shorter pulse duration, since the optical damage at short pulse regime depends on the energy flux and not power flux.

One may estimate the laser energy required to switch one SPL gap, with a 5 ps laser pulse on a ring cathode of 1 cm^2 area. If the current needed is 100 kA and the grainy yttrium cathode efficiency is 0.25%, the laser pulse energy needed would be under 1 mJ.

Excimer (KrF^*) lasers yielding 1 Joule in a few picoseconds would in theory be able to energize 1000 gaps of the SPL.

The electron bunch source at the center of the first SPL gap could utilize a smooth cathode and a metal with higher ϕ_0, since the fields there are expected to be in the 10^9 V/m range, and electron emission with low emittance is required.

Extension of our small area results to the 1 cm^2 area of the SPL ring shaped cathode, operation at high pulsed fields, the photoemission duration at fields near the field emission regime, as well as cathode life times, all remain to be explored. At the SPL, provisions have to be made for periodic rejuvenation of the cathode, e.g., by laser reactivation, or by thermionic heating if high melting temperature materials are considered.

ACKNOWLEDGEMENTS

We would like to acknowledge the support and valuable discussions with Drs. Veljko Radeka, Robert Palmer and Bill Willis. The SEM photos were prepared by Dr. John Warren. We appreciate the expert technical assistance of Neil Schaknowski and Michael Stuff and thank Barbara Kponou for the patient preparation of the manuscript.

REFERENCES

1. W. Willis, "Switched Power Linac," in C. Joshi and T. Katsouleas, Eds., *Proc. 2nd on Laser Acceleration of Particles Conf.* (Los Angeles, CA, January 7-18, 1985) AIP Conf. Proc. 130, p. 242.

2. R. B. Palmer, "The Microlasertron," SLAC-PUB-3890 Rev., Stanford Linear Accelerator, Stanford University, Palo Alto, CA, 1986.

3. R. C. Fernow, "Facilities for New Acceleration Techniques," in F. E. Mills, Ed., *Proceedings of the Advanced Accelerator Concepts Conference.* (Madison, WI, January 1986) AIP Conf. Proc. 156, p. 37.

4. K. Batchelor, et al., "The Brookhaven Accelerator Test Facility," presented at the 1988 Linear Accelerator Conference, Williamsburg, VA, October 3-7, 1988, (BNL-42020).

5. K. T. McDonald, "Design of the Laser-Driven RF Electron Gun for the BNL Accelerator Test Facility," DOE/ER/3072-43, Princeton University, Princeton, NJ, March 1988.

6. J. S. Fraser, R. L. Sheffield, et al., "Photocathodes in Accelerator Applications," in E. R. Lindstrom and L. S. Taylor, Eds., *Proc. 1987 IEEE Particle Accelerator Conf.* (Washington, DC, 1987) p. 1705.

7. C. K. Sinclair and R. H. Miller, "A High Current, Short Pulse, RF Synchronized Electron Gun for the Stanford Linear Accelerator," *IEEE Trans. Nucl. Sci.*, NS-28, 2649 (1981).

8. J. Fischer and T. Srinivasan-Rao, "UV Photoemission Studies of Metal Photocathodes for Particle Accelerators," presented at IV Workshop on Pulse Power Techniques for Future Accelerators, Erice, Italy, March 4-9, 1988, (BNL-42151).

9. M. Boussoukaya, et al., "Photoemission and Photofield Emission: Some Results," in J. B. Murphy and C. Pellegrini, Eds., *Proc. of ICFA Workshop on Low Emittance* $e^- - e^+$ *Beams* (Brookhaven National Laboratory, Upton, NY, March 20-25, 1987 - BNL 52090) p. 164.

10. J. Fischer and T. Srinivasan-Rao, "Short-Pulse High-Current-Density Photoemission in High Electric Fields," in S. Turner, Ed., *Proc. Workshop on New Developments in Particle Acceleration Techniques* (Orsay, France, 1987 - CERN 87-11, ECFA 87/110) Vol. 1, p. 506.

11. S. W. Downey, et al., "Simple Laser Driven Photocathode Electron Source," *Appl. Phys. Lett.* 49, 911 (1986).

12. W. F. Krolikowski, "Photoemission Studies of the Noble Metals, the Cuprous Halides, and Selected Alkali-Halides," PhD Dissertation, Stanford University, 1967 (University Microfilms, Ann Arbor, MI, 1968).

13. J. Knott, "Feasibility Studies for the Switched Power Linac," in S. Turner, Ed., *Proc. Workshop on New Developments in Particle Acceleration Techniques* (Orsay, France, 1987 - CERN 87-11, ECFA 87/110) Vol. 1, p. 336.

14. *CRC Handbook of Chemistry and Physics*, R. C. Weast, ed., Boca Raton, FL: CRC Press, 1979.

15. J. R. Stevenson and E. B. Hensley, "Thermionic and Photoelectric Emission from Magnesium Oxide," *J. Appl. Phys.* 32, 166, 1961.

16. P. May, J.-M. Halbout and G. Chiu, "Laser Pulsed e Beam System for High Speed IC Testing" in *Picosecond Electronics and Optoelectronics*, F. J. Leonberger, C. H. Lu, F. Capasso and H. Morkoc, Eds. New York, NY: Springer-Verlag, 1987, Vol II, p. 54.

17. M. Cordona and L. Ley, "Photoemission in Solids" in Topics in Applied Physics, M. Cordona and L. Ley, Eds. New York, NY: Springer-Verlag, 1978, Vol. 26, p..

18. M. Boussoukaya et al., "Emission de photocourants à partir de photocathodes à pointes," LAL RT/86-04, LAL, Orsay, France, March 1986.

19. W. Schottky, "Cold and Hot Electron Discharge," (in German) *Z. Phys.* 14, 63 (1923).

20. R. H. Fowler and L. Nordheim, "Electron Emission in Intense Electric Fields," in *Proc. Royal Soc.* A119, 173 (1928).

21. R. Hawley, "Electron Emission from Metallic Surfaces" in High Voltage Technology, L. L. Alston, Ed. Oxford, England, Oxford University Press, 1968. pp. 97 and 101.

22. R. H. Good and E. W. Müller, "Field Emission," *Encyclopedia of Physics*, 21, 176 (1956).

23. G. Y. Farkas, in *Multiphoton Processes*, J. H. Eberly and P. Lambropoulos, Eds. New York, NY: Wiley, 1978, p. 81.

24. T. Srinivasan-Rao, J. Fischer and T. Tsang, "Picosecond Photoemission from Microstructures," presented at the 1989 Workshop on Advanced Accelerator Concepts, Lake Arrowhead, CA, January 9-13, 1989.